Research Article Adv. Mat. Lett. 2013, **4**(9), 708-713 ADVANCED MATERIALS *Letters*

www.amlett.com, www.amlett.org, DOI: 10.5185/amlett.2013.1412

Polypropylene-nanoclay composites containing flame retardant additive: Thermal stability and kinetic study in inert atmosphere

Narender Kumar, J. B. Dahiya*

Department of Chemistry, Guru Jambheshwar University of Science & Technology, Hisar 125001, Haryana, India

*Corresponding author. Tel: (+91) 1662 263356; Fax: (+91) 1662 276240; E-mail: jbdic@yahoo.com

Received: 30 January 2013, Revised: 12 March 2013 and Accepted: 17 March 2013

ABSTRACT

Thermal degradation and stability of polypropylene-nanoclay composites containing organic phosphinate (OP) and ammonium polyphosphate (AP) flame retardants with maximum total 20 per cent loading was carried out using thermogravimetry (TG) and differential scanning calorimetry (DSC) analyses in inert atmosphere. Kinetic methods such as Broido, Horowitz-Metzger and Coats-Redfern were applied to study the mechanism of degradation of materials. The thermal stability of PP/PPgMA/AP/15A nanocomposite containing total 20 per cent loading is increased by 20 ^{o}C in comparison to that of control sample and also gives high char yield (14.4 %) due to presence of exfoliated clay and phosphorylating effect of AP in condensed phase. The random nucleation (first order) mechanism is found the most probable mechanism for PP composites degradation from kinetic study. The future prospective of the study is to develop superior fire safe polymeric materials. Copyright © 2013 VBRI press.

Keywords: Polypropylene; nanoclay; flame-retardant; thermogravimetry; kinetics.

Introduction

Thermoplastic polymers including polypropylene melt and drip on heating and lose their strength. On further heating they being organic in nature burn completely and leave no residue, which limit their use in wider and varied applications. Thermoplastic polymers have advantages to form composites and nanocomposites easily with desired and suitable inorganic and organic additives by melt blending method which is industrially viable and cost effective. Nanotechnology is a new generic approach for improved properties as compared to conventional technology by making use of nanosized materials which are environmental friendly **[1-3]**. Polymer nanocomposites have become an expanding field of research due to their outstanding improved properties over their pure polymeric materials such as thermal stability, heat and gas barrier, mechanical and flame retardancy **[4, 5]**. These improved properties are related to the dispersion of nanoparticles such as nanoclays in the polymer matrix and formation of nanostructure **[6]**. The very small amount of nanoclay is needed to improve remarkable properties due to their high aspect ratio **[7]**.

Polypropylene fibres are the fastest growing synthetic fibres for many applications such as automotive textiles, car industry, upholstery, wall coverings, home textiles, electrical cables, packaging and transportation. The large amount of conventional flame retardants is added to achieve the reasonable flame retardancy of polymers which makes the processing difficult particularly in case of synthesis of polymer fibres. Therefore, recent research is motivated to include the nanoclays in very small amount along with conventional phosphorous based flame retardants having advantage to reduce the high loading, which is an essential requirement to remove difficulty in processing for formation of fibres.

In the present study with the objective to develop flame retardant polymeric materials to prevent fire hazards, the thermal degradation and stability in inert atmosphere of polypropylene-nanoclay composites containing organic phosphinate and ammonium polyphosphate flame retadants with maximum total 20 per cent loading was carried out using thermogravimetric (TG) and differential scanning calorimetry (DSC) analyses. In this study PPgMA was added as a compatibilizer to improve the exfolation of clays in polypropylene matrix. Toyota researchers have used PPgMA as compatibilizer polypropylene-clay nanocomposites with increased properties **[8]**. Kinetics of thermal degradation has also been the subject of extensive research to know the degradation mechanism of the polymeric materials. Therefore, three well-known kinetic methods such as Broido (BR) **[9]**, Horowitz-Metzger (H-M) **[10]** and Coats-Redfern (C-R) **[11]** were applied to determine kinetic parameters and mechanism of degradation of materials.

Experimental

Materials

Polypropylene (isotactic, Sigma Aldrich Co., India), polypropylene grafted maelic anhydride (Sigma Aldrich Co., India), Cloisite-Na (pristine form of montmorillonite, Southern Clay Products Inc., Germany), Closite 15A (sodium montmorillonite modified with dimethyl dehydrogenated tallow ammonium cation, Southern Clay Products Inc., Germany), Exolit OP 1230 (organic phosphinate, Clariant Inc., Germany) and Exolit AP 422 (ammonium polyphosphate, Clariant Inc., Germany) were used to prepare nanocomposites. Polypropylene, polypropylene grafted maelic anhydride, Cloisite-Na, Closite 15A, Exolit OP 1230 and Exolit AP 422 are represented as PP, PPgMA, Na, 15A, OP and AP, respectively.

Preparation of nanocomposites

Polypropylene nanocomposites were prepared by melt blending method using twin screw extruder. About 500g material of each sample was processed using extruder. The detail of method and conditions for preparation of polypropylene nanocomposites are given in our earlier study **[12]**.

Table 1. Some common solid state reactions mechanism and integral mechanism functions.

Reaction model Symbol	**Mechanism function, g(α)**	**Reaction model**
	Diffusion control	
D1	α^2	One dimensional, Parabolic law
D2	$\alpha+(1-\alpha)\ln(1-\alpha)$	Two dimensional, Valensi equation
D3	$[1-(1-\alpha)^{1/3}]^2$	Three dimensional, spherical symmetry; Jander equation
D4	$(1-2\alpha/3)-(1-\alpha)^{2/3}$	Three-dimensional, spherical symmetry; Ginstling-Brounnstein equation
	Random nucleation and growth	
F1	$-\ln(1-\alpha)$	One nucleus on each particle; Mampel equation (first order)
A2	$[-\ln(1-\alpha)]^{1/2}$	Avrami equation I
A3	$[-\ln(1-\alpha)]^{1/3}$	Avrami equation II
	Phase boundary reaction	
R1	$1-(1-\alpha)$	Plate symmetry
R2	$1-(1-\alpha)^{1/2}$	Cylindrical symmetry
R3	$1-(1-\alpha)^{1/3}$	Spherical symmetry

Thermal analysis

Thermogravimetric analyses (TG) of PP nanocomposite samples were carried out in inert atmosphere (100 mL/min) with Thermogravimetric analyser at heating rate of 10 °C/min with a sample weight of about 5-10 mg. DSC analysis was carried out using a TA instruments DSC Q−10 differential scanning calorimeter thermal analyzer. About 4−8 mg of samples were weighed in the aluminum pan and placed in the DSC cell. The samples were then heated from 40 to 500 °C at a heating rate of 10 °C/min in inert atmosphere of nitrogen (50 mL/min).

Kinetic study

Kinetics study is an important tool to study the decomposition mechanism of the materials. Several kinetic methods in solid state Chemistry for calculating kinetic parameters depending on both experimental conditions as well as mathematical treatment of data have been reported in literature **[13-15]**. Some of these solid state reactions models are given in **Table 1**.

The kinetics of a reaction depends on the slowest step, which is the rate determining step. In solid state reactions (i) the nucleation and growth of product phase, (ii) diffusion controlled or (iii) reactions at phase boundary can be rate determining steps. Kinetics of solid-state reactions in non-isothermal conditions is usually calculated by the Arrhenius-type equation as-

$$\frac{d\alpha}{dT}=\frac{A}{\beta}exp\left[-\frac{E}{RT}\right]f(\alpha) \qquad \text{------- (1)}$$

Where α is the conversion factor, t is the time, *A* is the pre-exponential factor, *β* is the linear heating rate, *E* is the activation energy, *T* is the temperature and f(α) is the function that represent the reaction model.

In non-isothermal condition, the conversion factor (α) is given by-

$$\propto=\frac{m_o-m_t}{m_o-m_\infty} \qquad \text{------- (2)}$$

Where, m_o is the initial sample weight, m_t is the sample weight at time t, m_∞ is the final sample weight.

The three well-known kinetic methods such as Broido (BR), Horowitz- Metzger (H-M) and Coats-Redfern (C-R) methods are applied in this study and their main equations are given below:

1. Broido (BR) method

Mathematical form of BR method is

$$ln[-ln(1-\propto)]=-\frac{E}{RT}+ln\left[\frac{ART_s^2}{E\beta}\right] \qquad \text{------- (3)}$$

R is the gas constant, T is the absolute temperature at particular weight loss, *A* is the pre-exponential factor, β is the linear heating rate, T_s is the temperature at maximum degradation rate.

2. Horowitz- Metzger (H-M) method

Mathematical form of H-M method is

$$ln[-ln(1-\alpha)] = \frac{E\theta}{RT^2} \qquad \text{------- (4)}$$

Where $\theta = T\text{-}T_s$ which is the auxillary temperature variable.

3. Coats-Redfern (C-R) method

The C-R method is the integral method and its mathematical form is

$$ln\left[\frac{g(\alpha)}{T^2}\right] = ln\left[\frac{AR}{\beta E}\right] - \frac{E}{RT} \qquad \text{------- (5)}$$

This is the integral form of non-isothermal rate law where g(α) is the integrated from of various kinetic model equation as given in **Table 1**.

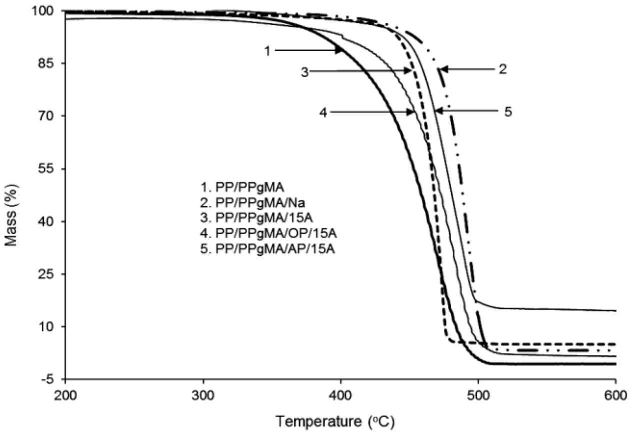

Fig. 1. TG curves of PP/PPgMA and its nanocomposites in inert atmosphere.

Results and discussion

Thermal study

The thermal analysis gives information on thermal stability and degradation behavior of the materials. The TG curves of the PP nanocomposites samples are shown in **Fig. 1**.

The TG data are given in **Table 2**, which include the temperatures at which 5 % ($T_{5wt\%}$), 10 % ($T_{10wt\%}$), 50 % ($T_{50wt\%}$) degradation occurs, DTG peaks and the char yield at 550 ^{0}C in inert atmosphere. The DSC curves of samples are shown in **Fig. 2**.

Table 2. TG data of PP/PPgMA and its nanocomposites in inert atmosphere.

Composite sample	Stages/ Temp. Range (°C)	Wt Loss (%)	$T_{5wt\%}$ (°C)	$T_{10wt\%}$ (°C)	$T_{50wt\%}$ (°C)	DTG peak (°C)	Char yield at 550 °C (%)
PP/PPgMA (90+10)*	1st/0-358	3.0	374	397	457	468	0.0
	2nd/358-500	96.1					
PP/PPgMA/Na (85.5+9.5+5)	1st/0-415	2.3	442	461	488	492	3.2
	2nd/415-515	94.1					
PP/PPgMA/15A (85.5+9.5+5)	1st/0-432	4.6	434	446	468	471	5.0
	2nd/432-476	86.5					
PP/PPgMA/OP/15A (72+8+15+5)	1st/0-400	7.0	376	415	471	470	1.9
	2nd/400-505	88.8					
PP/PPgMA/AP/15A (72+8+15+5)	1st/0-420	3.6	433	450	480	487	15.0
	2nd/420-500	79.4					

* Composition of nanocomposites is given in small parenthesis.

The initiation maximum and final temperatures of DSC peaks and heat involved are given in **Table 3**.

Table 3. DSC data of PP/PPgMA and its nanocomposites in inert atmosphere.

Composite sample	DSC temperature (°C)			Heat flow (J/g)	Nature of peak
	Initiation	Maximum	Final		
PP/PpgMA	150	162	172	101	Endo
	418	456	490	493	Endo
PP/PpgMA/Na	152	162	177	76	Endo
	424	462	485	464	Endo
PP/PpgMA/15A	152	162	168	72	Endo
	439	450	471	519	Endo
PP/PPgMA/OP/15A	152	163	171	59	Endo
	423	465	501	616	Endo

TG curve of PP/PPgMA sample shows two stages of thermal degradation in the temperature range upto 358 °C and 358 to 500 ^{O}C. The PP/PPgMA degrades almost completely by leaving no char residue at 550 ^{O}C. Second stage of thermal degradation is the major stage of degradation with 96.1 % wt. loss and supported by DTG peak at 468 ^{O}C. The DSC peak of this sample gives two endotherms with maxima at 162 and 456 ^{O}C in inert atmosphere. The first endotherm corresponds to the melting of the polymer with the heat transition of 101 J/g. The second endotherm is due to its major decomposition of PP/PPgMA involving heat transition of 493 J/g.

Effect of clays

TG curves of PP/PPgMA/Na and PP/PPgMA/15A containing 5 wt% each of pristine clay (Na) and organic modified clay (15A) show similar stages of degradation but with the increase of thermal stability and char yield in comparison to PP/PPgMA control. **Table 2** reveals that

PP/PPgMA/Na nanocomposite has higher values of temperatures ($T_{5wt\%}$, $T_{10wt\%}$ and $T_{50wt\%}$) of degradation and also higher DTG peak maxima in comparison to that of PP/PPgMA/15A indicating that the structure of PP/PPgMA/Na nanocomposite with pristine clay (Na) is more thermally stable by 20 ^{O}C than the nanocomposite containing organically modified clay (15A). But the char yield at 550 ^{O}C in case of PP/PPgMA/15A is found higher than that of PP/PPgMA/Na although they contain same amount of clays. The TG curve of PP/PPgMA/15A (**Fig. 1**) shows that this nanocomposite destabilizes in comparison to PP/PPgMA beyond 472 ^{O}C indicating the collapse of nanocomposite structure. But PP/PPgMA/15A gives higher char yield in comparison to PP/PPgMA and PP/PPgMA/Na, which indicates that the organoclay is more interactive and provides more efficient barrier at very high temperature to prevent the volatiles to escape into combustion phase in comparison to pristine clay. DSC curves of PP/PPgMA/Na and PP/PPgMA/15A show peaks similar to the PP/PPgMA except that the second endotherm of PP/PPgMA/15A due to the decomposition is very sharp and occurs at low temperature involving more heat (519 J/g).

Effect of clay and organic phosphinate

Table 2 reveals that PP/PPgMA/OP/15A nanocomposite starts degradation at lower temperature in comparison to PP/PPgMA/15A, which may be due to catalytic degradation of polymer by phosphonic acid released on decomposition of organic phosphinate (OP) flame retardant. The TG curve of PP/PPgMA/OP/15A in inert atmosphere shows that it does not degrade as rapidly as PP/PPgMA/15A after a temperature of about 50% weight loss, which may be due to formation of polyphosphoric acid and metal phosphate **[12,16]**. This is supported by second endotherm peak in DSC curve of PP/PPgMA/OP/15A [**Fig. 2**] in inert atmosphere, which appears at higher temperature (465 ^{O}C) involving greater heat of value 616 J/g in comparison to PP/PPgMA/15A. The PP/PPgMA/OP/15A nanocomposite containing 15 wt% OP gives little char yield (1.9%) indicating that most of OP and products obtained on decomposition of OP vaporize to gaseous phase **[16]**. The thermal study of PP composites containing OP infers that OP flame retardant acts in vapour phase and not in the condensed phase.

Effect of clay and ammonium polyphosphate

The TG curve of PP/PPgMA/AP/15A (**Fig. 1**) shows 3.6% weight loss upto 420 ^{o}C and further 79.4% weight loss occurs in small temperature range 420-500 ^{o}C. The $T_{5wt\%}$, $T_{10wt\%}$ and $T_{50wt\%}$ (**Table 2**) of PP/PPgMA/AP/15A are observed higher in comparison to that of PP/PPgMA control sample, PP/PPgMA/15A and PP/PPgMA/OP/15A except PP/PPgMA/Na. The increase in thermal stability of PP/PPgMA/AP/15A is also supported by DTG maximum observed at 487 ^{O}C in comparison to that of control sample (468 ^{O}C). The ammonium polyphosphate (AP) decomposes initially and gives ammonia and phosphoric acid. Later the released phosphoric acid polymerizes and cross links at higher temperature resulting the thermal stable structure **[5]**. The PP/PPgMA/AP/15A composite shows highest char yield value of 14.4 % due to presence of exfoliated clay and phosphorylating effect of AP in condensed phase. The char residue formed may be able to hinder diffusion of low molecular weight volatiles as well as insulates the underlying polymer from heat and air atmosphere.

Table 4. Kinetic parameters of PP/PPgMA and its nanocomposites by Broido and Horowitz-Metzger method.

Composite sample	**Broido Method**			**Horowitz-Metzger Method**	
	E (kJ/mol)	*R*^{2}	*A* (min^{-1})	*E* (kJ/mol)	*R*^{2}
PP/PPgMA	151.9	0.9841	1.91×10^{10}	163.4	0.9913
PP/PPgMA/Na	379.4	0.9881	6.83×10^{25}	391.1	0.9910
PP/PPgMA/15A	448.7	0.9776	3.7×10^{31}	462.0	0.9806
PP/PPgMA/OP/15A	176.7	0.9746	7.81×10^{11}	184.5	0.9831
PP/PPgMA/AP/15A	318.0	0.9991	7.03×10^{21}	338.8	0.9995

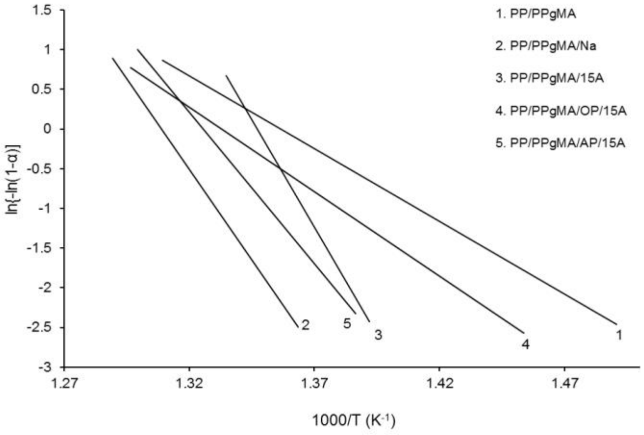

Fig. 3. Plot of ln[-ln(1-α)] versus 1000/T using Broido's method.

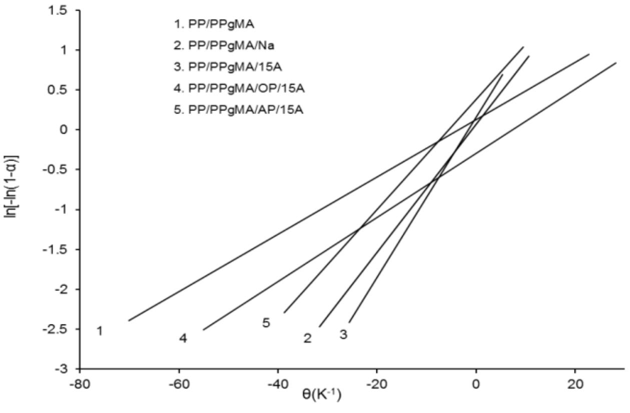

Fig. 4. Plot of ln[-ln(1-α)] versus θ using Horowitz-Metzger method.

Kinetic study

Kinetic parameters for thermal degradation of polypropylene nanocomposite samples were evaluated by Broido, Horowitz-Metzger and Coats-Redfern methods. The values of activation energy (*E*), pre-exponential factor (*A*) and correlation coefficient (R^2) were calculated for the conversion in the range $\alpha = 0.1$ to 0.95 for their major stage of degradation at constant single heating rate of 10

^{O}C/min. Kinetic parameters (E and A) of PP nanocomposites obtained by BR and H-M methods are given in **Table 4**. The kinetic parameters obtained by C-R method for PP nanocomposites are listed in **Tables 5 & 6**. The plots of ln[-ln(1-α)] versus 1000/T (BR method), ln[-ln(1-α)] versus β (H-M method) and ln[-ln(1-α)]/T^2] versus 1000/T (C-R method) for major stage of degradation of the samples are shown in **Figs. 3, 4 & 5**, respectively.

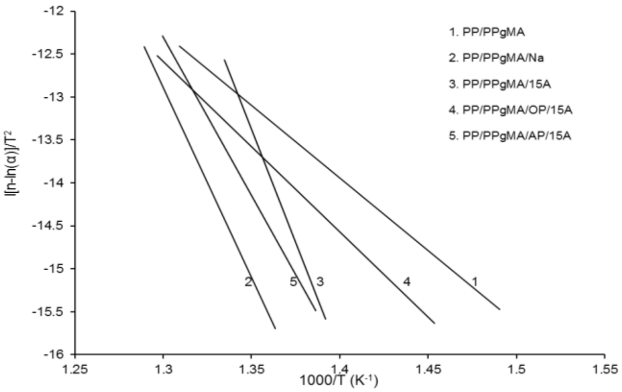

Fig. 5. Plot of ln[-ln(1-α)]/T^2 versus 1000/T using Coats-Redfern method (Random nucleation, first order).

The aim of kinetics is to obtain information about decomposition mechanism through comparison of a series of measured values of degree of conversion (α) with time (t) and the functional relationship between α and t derived from models given in **Table 1**. Generally identification of kinetic model for the reaction is determined by the best linearity of a plot of g(α) versus time i.e. highest value of regression coefficient (R^2). But **Tables 5 & 6** of C-R method reveals that all reaction models for PP/PPgMA, PP/PPgMA/Na, PP/PPgMA/15A, PP/PPgMA/OP/15A, PP/PPgMA/AP/15A show high regression coefficient (R^2) values i.e. more than 0.96 and also all values are very close for their major stage of degradation ($\alpha = 0.1$ to 0.95). Therefore, it is not appropriate to decide reaction model of thermal degradation of samples on the basis of R^2 only rather all three kinetic parameters (E, A and R^2) should be taken into account. On the basis of pre-exponential factor value in case of PP/PPgMA, the nucleation models (A2 and A3) have very small values of pre-exponential factor which are out of appropriate range of pre-exponential factor values 10^6-10^{18} sec^{-1} **[17]**. Therefore, the nucleation models (A2 and A3) can not be considered the correct reaction mechanism. The remaining F1, D1, D2, D3, D4, R1, R2 and R3 models have values of A in appropriate range (10^6-10^{18} sec^{-1}) and also have maximum absolute value of regression coefficient thus these models can be considered the probable reaction mechanism models in case of PP/PPgMA. Further, on comparing activation energies (**Table 5**) of these different models obtained using C-R based method with the activation energies 151.9 and 163.4 kJ/mol (**Table 4**) obtained by BR and H-M methods, respectively, the random nucleation-first order (F1) mechanism has comparable value of activation energy (140.7 kJ/mol). Thus random nucleation-first order (F1) is the most probable reaction mechanism of PP/PPgMA degradation. Similarly on the basis of three parameters E, A and R^2 and comparing activation energy with the energy values obtained by other BR and M-H methods, the probable reaction mechanism model are suggested for other PP nanocomposite samples.

Table 5. Kinetic parameters of PP/PPgMA, PP/PPgMA/Na and PP/PPgMA/15A by Coats-Redfern method.

Reaction model symbol	**Composite sample**								
	PP/PPgMA			PP/PPgMA/Na			PP/PPgMA/15A		
	E (kJ/mol)	R^2	A (min^{-1})	E (kJ/mol)	R^2	A (min^{-1})	E (kJ/mol)	R^2	A (min^{-1})
D1	207.1	0.9978	7.3×10^{13}	539.2	0.9953	2.7×10^{36}	654.0	0.9996	5.4×10^{45}
D2	230.3	0.9979	2.4×10^{15}	595.6	0.9969	1.4×10^{40}	717.8	0.9974	1.2×10^{50}
D3	260.4	0.9926	1.2×10^{17}	667.8	0.9946	4.6×10^{44}	798.3	0.9897	1.9×10^{55}
D4	240.2	0.9968	3.2×10^{15}	619.3	0.9967	1.6×10^{41}	744.2	0.9954	2.3×10^{51}
F1	140.7	0.9809	2.9×10^{9}	366.9	0.9873	9.2×10^{24}	436.6	0.9765	5.0×10^{30}
A2	64.4	0.9776	5.2×10^{3}	177.1	0.9865	4.7×10^{11}	212.1	0.9752	3.9×10^{14}
A3	38.9	0.9735	4.9×10^{1}	113.9	0.9856	1.4×10^{7}	137.3	0.9738	1.4×10^{9}
R1	97.5	0.9975	1.0×10^{6}	263.3	0.9951	3.1×10^{17}	320.9	0.9996	1.6×10^{22}
R2	116.8	0.9955	1.8×10^{7}	309.8	0.9962	3.6×10^{20}	373.2	0.9938	5.6×10^{25}
R3	124.2	0.9921	4.8×10^{7}	327.6	0.9944	4.6×10^{21}	393.0	0.9894	1.0×10^{27}

The F1 mechanism is found the most probable mechanism in all PP/PPgMA composites. Further, the value of activation energy for PP/PPgMA/Na nanocomposite (366.9 kJ/mol) degradation is observed more than double in comparison to PP/PPgMA (140.7 kJ/mol) and it further increased in PP/PPgMA/15A nanocomposite (436.6 kJ/mol) indicating their increased thermal stability due to formation of nanocomposite structure. The activation energy in case of PP/PPgMA/OP/15A is found in the range of control sample which may be due to decomposition and vaporization of OP and also catalyzed degradation of PP. This is also supported by TG data (**Table 2**). The activation energy for PP/PPgMA/AP/15A degradation is found higher than PP/PPgMA/OP/15A because AP forms polyphosphoric acid and cross linked stable structure **[5]** on heating. The increased cross linking is also indicated by the formation higher char yield.

Table 6. Kinetic parameters of PP/PPgMA composites containing FRs by Coats-Redfern method.

Reaction model symbol	**Composite sample**					
	PP/PPgMA/OP/15A			PP/PPgMA/AP/15A		
	E (kJ/mol)	R^2	A (min^{-1})	E (kJ/mol)	R^2	A (min^{-1})
D1	246.6	0.9955	2.7×10^{16}	441.2	0.9829	1.1×10^{30}
D2	272.4	0.9930	1.2×10^{18}	490.5	0.9921	2.2×10^{33}
D3	305.4	0.9853	9.0×10^{19}	554.3	0.9987	2.1×10^{37}
D4	283.2	0.9910	1.8×10^{18}	511.4	0.9951	1.6×10^{34}
F1	164.6	0.9712	1.0×10^{11}	305.6	0.9991	9.5×10^{20}
A2	76.2	0.9670	3.3×10^{4}	146.6	0.9990	4.4×10^{9}
A3	46.8	0.9618	1.8×10^{2}	93.6	0.9989	6.0×10^{5}
R1	117.2	0.9951	2.1×10^{7}	214.4	0.9819	1.8×10^{14}
R2	138.5	0.9998	4.9×10^{8}	255.2	0.9962	9.5×10^{16}
R3	146.6	0.9842	1.4×10^{9}	270.9	0.9986	9.0×10^{17}

Conclusion

Thermal degradation and stability of polypropylene-nanoclay composites containing organic phosphinate (OP) and ammonium polyphosphate (AP) flame retardants was carried out in inert atmosphere. The thermal study of polypropylene composites containing OP infers that OP acts in vapour phase and AP acts in condensed phase. The thermal stability of PP/PPgMA/AP/15A nanocomposite containing total 20 per cent loading is increased by 20 ^{o}C in comparison to that of control sample and also gives high char yield (14.4 %) due to presence of exfoliated clay and phosphorylating effect of AP. The value of activation energy for PP/PPgMA/Na and PP/PPgMA/15A composites degradation is increased more than double in comparison to PP/PPgMA indicating their increased thermal stability due to formation of nanocomposite structure. The random nucleation (first order) mechanism is found the most probable mechanism for PP composites degradation from kinetic study.

Acknowledgements
The authors (J. B. Dahiya and Narender Kumar) are grateful to the UGC, New Delhi, for the financial support for this work.

Reference

1. Kumar, S.; Shinde, T. J.; Vasambekar, P. N. *Adv. Mat. Lett.* **2013**, 4,373.
   DOI: 10.5185/amlett.2012.10429.
2. Tiwari, A. *Adv. Mat. Lett.* **2012,** 3,1.
   DOI: 10.5185/amlett.2012.13001.
3. Tiwari, A.; Mishra, A. K.; Kobayashi, H.; Turner, A. P. F. In *Intelligent Nanomaterials;* Wiley-Scrivener Publishing, USA,
   ISBN: 978-04-709387-99, 2012.
4. Wilkie, C. A.; Morgan, A. B. In *Advances in fire retardant materials;* Horrocks, A. R.; Price, D. (Eds.); Woodhead Publishing Ltd; 2008.(pp 95-123).
5. Dahiya, J. B.; Rathi, S.; Bockhorn, H.; Haußmann, M.; Kandola, B. K. *Polym. Degrad. Stab.* **2012**, 97, 1458.
   DOI: 10.1016/j.polymdegradstab.2012.05.012.
6. Morgan, A. B.; Gilman, J. W. *J. Appl. Polym. Sci.* **2003**, 87, 1329.
   DOI: 10.1002/app.11884.
7. Qin, H.; Zhang, S.; Zhao, C.; Feng, M.; Yang, M.; Shu, Z.; Yang, S. *Polym. Degrad. Stab.* **2004**, 85, 807.
   DOI: 10.1016/j.polymdegradstab.2004.03.014.
8. Nam, P. H.; Maiti, P.; Okamoto, M.; Kotaka, T.; Hasegawa, N.; Usuki, A. *Polymer* **2001**, 42(23), 9633.
   DOI: 10.1016/S0032-3861(01)00512-2.
9. Broido, A. *J. Polym. Sci.*, Part A-2, **1969**, 7, 1761.
   DOI: 10.1002/pol.1969.160071012.
10. Horowitz, H. H.; Metzger G. *Anal. Chem.* **1963,** 35, 1464.
    DOI: 10.1021/ac60203a013.
11. Coats, A. W.; Redfern, J. P. *Nature.* **1964,** 201, 68.
    DOI: 10.1038/201068a0.
12. Dahiya, J. B.; Kumar, N.; Bockhorn, H. *Fire and Materials*.
    DOI: 10.1002/fam.2151.
13. Brown, M. E.;Galwey, A. K. In *Thermal Decomposition of Ionic solids*, Elsevier, Amsterdam, (1999) p. 75.
14. Dahiya, J. B.; Kumar, K.; Hagedorn, M. M.; Bockhorn, H. *Polym. Int.* **2008,** 57, 722.
    DOI: 10.1002/pi.2398.
15. Conesa, J. A.; Marcilla, A.; Caballero, J. A.; Font, R. *J. Anal. Appl. Pyrol.* **2001,** 58/59, 617.
    DOI: 10.1016/S0165-2370(00)00130-3.
16. Braun, U.; Schartel, B. *Macromol. Mater. Eng.* **2008**, 293, 206.
    DOI: 10.1002/mame.200700330.
17. Vyazovkin, S.; Wight, C. A. *Int. Rev. Phys. Chem.* **1998,**17(3), 407.
    DOI: 10.1080/014423598230108.